Jestr

Journal of Engineering Science and Technology Review 15 (1) (2022) 85 - 92

JOURNAL OF
Engineering Science and Technology Review

Research Article

www.jestr.org

Stiffness Degradation Law of Prestressed Concrete Beams under Equivalent Fatigue Loads

Qin Xin[1,2,*], Xiuquan Hu[1], Yuanwen Zhang[1,2], Erzhong Chen[1,2] and Ruyu Gao[1]

[1]*School of Civil Engineering, Hebei University, Baoding 071002, China*
[2]*Technology Innovation Center for Testing and Evaluation in Civil Engineering of Hebei Province, Hebei University, Baoding 071002, China*

Received 17 January 2022; Accepted 1 April 2022

Abstract

With the increase in bridge operation life and the effect of vehicle load, the property of bridge especially the reciprocating effect of heavy-load traffic, which endangers the safety of bridge operation, will be degraded. To further clarify the relationship between the stiffness and fatigue damage under heavy traffic, six prestressed concrete fatigue test beams were designed and manufactured. The equivalent fatigue load was determined by the statistics of traffic flow data. On the basis of the fatigue damage principle, the fatigue failure form and crack development of test beams under equivalent fatigue load were analysed. The constant-amplitude fatigue test method was employed to analyze the section stiffness degradation law and the member stiffness degradation law under equivalent fatigue load. Results demonstrate that the final failure mode of the test beam is the bending failure, which starts from the fatigue fracture of the longitudinal tensile steel bars at the bottom of the beam. With increased fatigue loading times, the stiffness of the test beams exhibits a three-stage decay trend of "fast–gentle–fast". The equivalent fatigue load accelerates the initial stiffness degradation of the prestressed beam, and the bridge design by the normal operating load is conservative. The section stiffness, which is characterized by the prestressed reinforcement strain, correlates best with the member stiffness of the beam. The proposed method provides a certain reference for the design, detection, and early warning of damage of bridge structures.

Keywords: Equivalent fatigue load, Heavy traffic, Stiffness, Constant-amplitude fatigue test

1. Introduction

The partially prestressed concrete (PPC) structural performance is between ordinary steel and fully prestressed concrete bridges and has high strength, good ductility, and other advantages [1]. The demand for the construction of PPC in roads and bridges has maintained an increasing trend and attracted the attention of scholars. Thus, experimental studies on prestressed concrete members have been conducted. At present, most studies on prestressed concrete beams focused on the fatigue life under the action of reciprocating fatigue load [2]. Scholars provided the fatigue life prediction formula of reinforced concrete members based on the stress amplitude of the steel bar [3]. The fatigue life prediction formula can guarantee the safety of components within a certain range. However, with the development of the transportation industry, the type of vehicle loads on highway bridges has also changed significantly, leading to problems, such as overlimit deformation and overlimit cracks in some components during the normal service period and threatening the operational safety of bridge structures [4]. According to survey data, the ownership of road trucks and the proportion of road freight in the total freight volume continues to rise, thus aggravating the overloading trend of road bridges and further leading to the cracking of bridge structures, reduction of effective prestress, and stiffness degradation [5-6].

For this reason, on the basis of the fatigue damage principle, scholars conducted studies on the stiffness degradation of the beam fatigue failure form and crack development under equivalent fatigue load [7]. A problem of deviation from the actual service status of the relationship is present. Therefore, how to accurately consider the fatigue characteristics of bridge structures under a load of actual operating vehicles should be urgently solved, and the development law of stiffness degradation should be clarified.

Therefore, in this study, the stiffness degradation law of prestressed concrete beams under equivalent fatigue load is elucidated using mathematical statistics and fatigue tests, and the stiffness degradation performance of the test beams is analyzed. This study aims to predict the optimal characterization parameters of bridge structure stiffness degradation under equivalent fatigue load accurately and provide a reference for the premonition of bridge fatigue failure.

2. State of the art

At present, scholars from China and other countries studied the fatigue performance of PPC bridge structures. Many scholars chose to use the finite element for damage analysis. The calculation model established by Vaško [8] can predict the damage of the beam under static load, whereas Wang [9] and others calculated the shrinkage and creep of concrete, the change of bridge stiffness, and the downward deflection caused by prestressing loss and conducted external prestress reinforcement analysis. Zhou [10] provided a feasible

*E-mail address: xinqin0902@163.com
ISSN: 1791-2377
doi:10.25103/jestr.151.11

method and theoretical basis for the accurate evaluation of local fatigue damage accumulation of bridge structures. Allawi [11-12] studied the flexural capacity of reinforced concrete beam members after fatigue load through tests and numerical analysis methods, but a detailed study and analysis on the ductility after failure are lacking. The feasibility of predicting the degradation of the bridge structure based on the grey theory needs to be verified by considering the actual degradation range of the bridge stiffness [13]. Garavaglia [14] used the Monte Carlo numerical method to simulate the variation of residual resistance section and an ultimate bending moment of the bridge deck with time. Similarly, OBrien [15-16] simulated the load effect of the bridge but ignored the complexity, such as the periodicity of traffic volume. Wang [17] studied the fatigue performance of key joints of composite beam bridges under the action of two trains from the two aspects of maximum stress amplitude and fatigue cumulative damage but did not study the reciprocating effect of heavy traffic. Xu [18] and others extracted the traffic flow distribution parameters, such as axle number, axle load, and wheelbase, through the MATLAB and established the vehicle load equivalent model on the basis of the equivalent principle of Miner linear accumulation damage and fatigue damage. However, due to the limitations of the current prestress state detection technology, the prestress loss of the real bridge is difficult to determine. To further deduce the calculation model of the section stiffness degradation of prestressed concrete beams after fatigue damage, Zhou [19] and others analyzed the experimental results of prestressed concrete beams with different sizes under multistage variable amplitude fatigue cyclic load and verified the accuracy of the stiffness degradation model. Nesterova [20] used the peak over threshold method to analyze the fatigue of the Milo viaduct deck. Bertolesi [21] used the full-scale test to test the railway steel riveted bridge, calibrated the elastic numerical model of the whole structure, and estimated the residual fatigue life of the bridge. Li [22] calculated the damage index of the stiffness degradation model on the basis of the quadratic pushdown analysis method. Zhang [23] and others found that the congenital defects existing in the construction stage are the main reason for the stiffness degradation of the bridge. Many fatigue tests [24-27] show that the fatigue failure of the PPC beam starts from nonprestressed reinforcement. The development of section stiffness affects the fatigue life of the beam directly, but minimal attention is paid to the optimal characterization parameters of the fatigue damage. Moreover, existing studies focused on the fatigue performance of prestressed concrete beams under normal operating load, and minimal consideration is given to the actual vehicle load. Therefore, the fatigue problem of PPC bridges under actual operation load should be studied.

Given the shortcomings of the existing research and focusing on the influence of the actual operation load, this study proposes an equivalent fatigue load suitable for the actual traffic volume and carries out the constant-amplitude fatigue test of the prestressed concrete beam under the equivalent fatigue load. The fatigue damage performance of prestressed concrete beams is analyzed from the two angles of stiffness attenuation of components and section stiffness attenuation, and parameters that can characterize the stiffness correlation are proposed to provide a reference for bridge design, monitoring, and detection.

The remainder of this study is organized as follows. Section 3 establishes the experimental design and the analysis of the test results. Section 4 proposes that the section stiffness of the beam, which is characterized by the prestressed steel bar strain, has the best correlation with member stiffness. Section 5 summarizes the conclusions.

3. Methodology

3.1 Experiment

In this test, six PPC beam specimens are made in the same batch, among which specimen S1 is subjected to a static load test to determine the ultimate load, and the remaining five specimens are subjected to a fatigue test and sequentially numbered as C1, C2, C3, C4, and C5. Figure 1 shows the cross-sectional dimensions of the specimen. By changing the stress amplitude of the equivalent fatigue load, the effect of the equivalent fatigue load on the failure form and stiffness degradation of the PPC beam is analyzed.

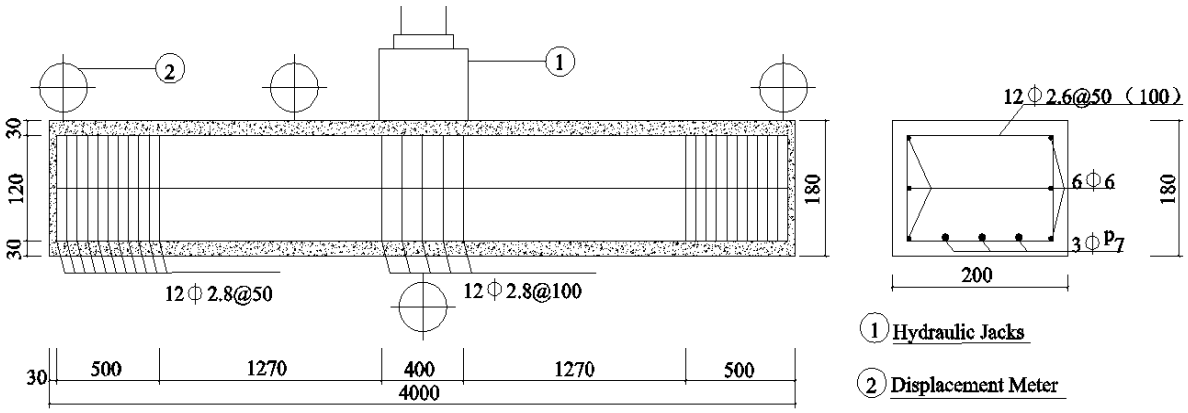

Fig.1 Cross-section reinforcement drawing and loading method [26]

Compressive strength and tensile tests are carried out on the test materials in accordance with the standard material property test requirements and methods specified in the standard “Standard for Mechanical Properties of Ordinary Concrete” and “Room Temperature Tensile Test Method for Metallic Materials”, respectively.

Test data are measured using different components [26]. The compressive strength of the test cube is 42.6 MPa. The axial compressive strength of the prism block is 29.8 MPa. The yield strength, ultimate strength, and elongation of prestressed steel wire are 1410 MPa, 1603 MPa, and 4.2%, respectively. The yield strength, ultimate strength, and

elongation of ordinary steel bars are 316 MPa, 420 MPa, and 25%, respectively.

The static test is conducted on the static load testing machine, and the ultimate bearing capacity is 23.8 kN. The fatigue test adopts concentrated force loading and sine wave loading at a frequency of 2 Hz. The measurement contents of this test include the displacement value of the loading point, concrete strain, steel bar strain, and prestressed tendon strain to understand the stiffness degradation law of the specimen. The test loading setup is shown in Figure 1.

In the fatigue test, a static load test is first performed on test beams C1–C5 to compare the changes in the mechanical properties of the specimens after fatigue loading. Before the static load test measurement, the strain gauge acquisition system needs to be reinitialized to eliminate the influence of self-weight.

3.2 Equivalent fatigue load

About 0.15 times the ultimate load is taken as the lower limit of the fatigue load [20]. The upper limit of fatigue load is determined in accordance with the statistical results of the actual traffic volume. A continuous 168-hour actual traffic flow survey is conducted at the site. In accordance with different axle types, heavy-duty vehicles are categorized into five types. At the same time, according to the principle of coaxial merging and the Miner criterion [25], the axle load is equivalently converted based on the principle of equal fatigue damage accumulation, and the load spectrum model of the heavy-duty vehicle is obtained (Table 1).

Figure 2 shows the maximum bending moment effect of the actual operating heavy-duty traffic vehicle load and highway class I vehicle load under the condition of simply supported beam bridges with different spans. The ratio of the bending moment effect (S_{ht})of the heavy traffic load in the actual investigation to the bending moment effect (S_0) of the highway-I level cycling load in the specification is defined as $\eta_i = S_{ht} / S_0$, where i represents different spans.

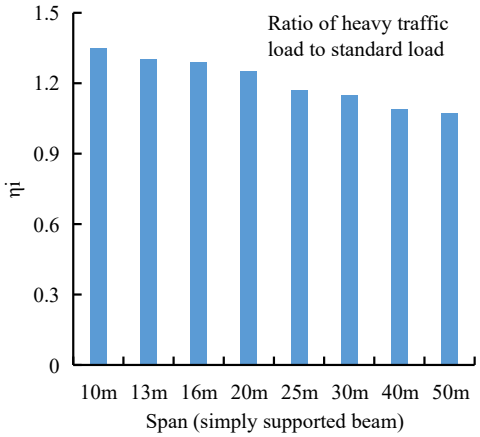

Fig.2 Heavy load and standard load action ratio.

Table 1. Heavy-duty vehicle load spectrum

Number of axes	Icon (Axle weight: kN Wheelbase: m)	Gross weight (kN)	Relative frequency
2	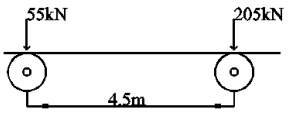	260	0.44
3	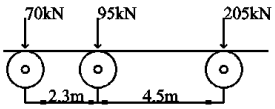	370	0.05
4	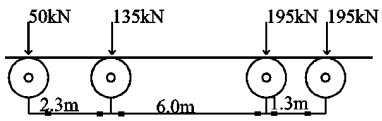	575	0.07
5	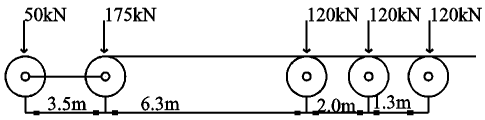	585	0.05
6	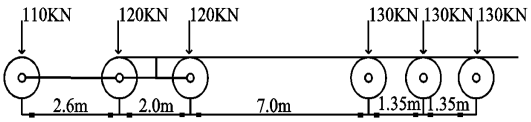	740	0.39

Statistics show that η_i is between 1.07 and 1.35. For a number of transportation routes with heavy traffic flow, the actual vehicle load on the current bridge is larger than the specified load. This result means that the current assessment of bridge fatigue damage is conservative through specification effect analysis, and the conclusion of bridge life assessment is dangerous. Taking a 16 m span beam as an example, $\eta_{16} = 1.29$, indicating that the actual operational traffic load (cars) is close to 1.29 times that of the road-I class load. Further considering the live load subitem factor of 1.5 and the importance factor of 1.1, the vehicle load effect is 2.1285 times that of the ultimate load of the bridge. The study of the heavy-load vehicle spectrum found that the vehicle load effect is about the ultimate load effect of the bridge. Therefore, in the case of ignoring the self-weight effect, according to the classification method commonly used in fatigue tests, the upper limit of the fatigue load

considering the overload effect should be taken as 0.56–0.84 M_u. Considering the randomness of the field survey data and the limitations of the laboratory, we have determined this range to be 0.5–0.8 M_u for the upper limit of the load during the fatigue load test of prestressed concrete beams to start with 0.50 times that of the ultimate load, and is divided into five, i.e., 0.5, 0.6, 0.7, 0.75, and 0.8 M_u.

4. Result Analysis and Discussion

4.1 Fatigue failure analysis

After 2 million fatigue cycles, test beams C1, C2, and C3 do not suffer from fatigue failure. The static load failure test is conducted on three specimens and shows that the failure mode is the bending failure. The fatigue failure of test beams C4 and C5 occur, and the fatigue life is 108,000 and 53,000 times, respectively. The failure starts from the fatigue fracture of the nonprestressed steel bar at the bottom of the beam, which occurs at the section of the main crack (near the loading point). The fracture is divided into an evident instantaneous break zone. Figure 3 shows the fatigue failure form.

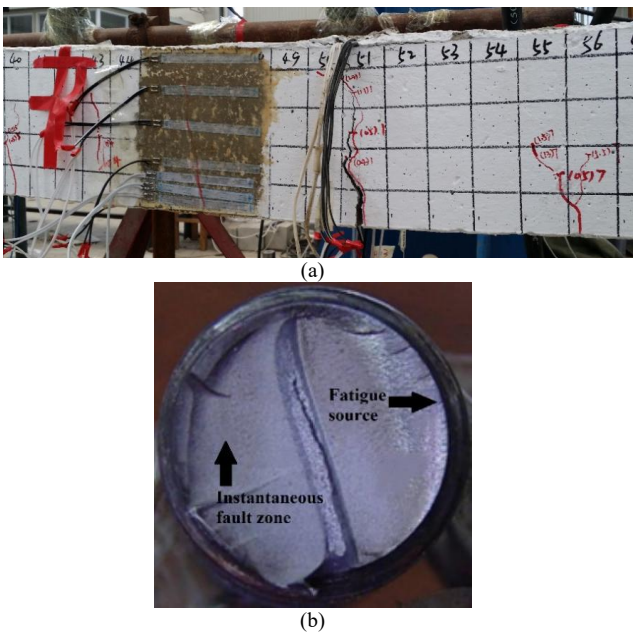

(a)

(b)

Fig. 3 The failure mode of specimens. (a) Fatigue bending failure shape. (b)Rebar fatigue fracture.

4.2 Stiffness degradation law

The variation characteristics of mid-span deflection (f) with the number of load cycles (N) reflect the development of cracks during the fatigue test and the change in the bond-slip properties of the interface between the reinforcement and concrete. The relationship between load and displacement is one of the comprehensive reflection factors of fatigue performance. Figure 4 shows the load– f curve of the test beam C4. The increase in the f of the test beam is related to the upper limit of fatigue and the number of fatigue loads. Except in the first loading, the deflection and load are not linearly related. Under other working conditions, the deflection and load are linear, and the load–deflection curve develops in a "loose–dense–loose" state.

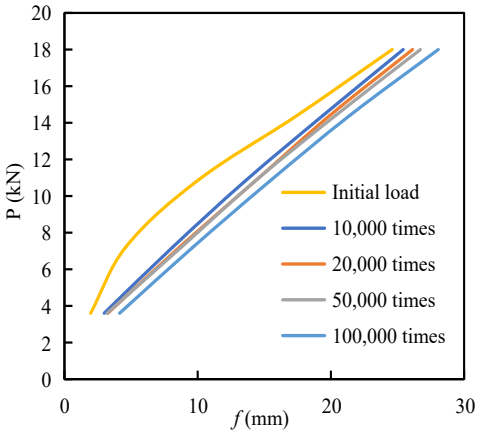

Fig. 4 Load deflection curves.

Stiffness refers to the ability of a material or structure to resist deformation and is an indication of how easily a material or structure deforms. In the inelasticity theory, stiffness is the force required to cause a unit displacement. The stiffness degradation coefficient (B_n / B_0) is proposed for the concrete simply supported beam under concentrated load to express the stiffness degradation intuitively. B_0 is the initial stiffness, and B_n is the stiffness of the specimen after n times of fatigue loading. In accordance with the test data of constant-amplitude fatigue test load–deflection change, the stiffness degradation curve of the test beam can be obtained (Figure 5).

Figure 5 shows that with increasing number of loads, B_n / B_0 decreases, the stiffness of the beam member is reduced, and the overall stiffness degradation presents staged characteristics. For the same number of fatigue loads and the same lower limit of fatigue load, the upper limit of fatigue load is increased, and the stiffness degradation of the test beam speeds up. For the test beam that has undergone 2 million fatigue loads and still has no fatigue damage, the stiffness degradation presents two-stage characteristics: rapid stiffness degradation in the initial stage of loading and steady decline in the middle stage. After the initial stiffness degradation, the B_n / B_0 values of the test beams before 100,000 times of fatigue loading are compared. Beams C1, C2, and C3 have little stiffness attenuation at the initial stage of fatigue loading. Beams C4 and C5 have fast stiffness decays and quickly reach failure, indicating that the overload effect accelerates the rapid degradation of the initial stiffness and the fatigue failure.

Figure 6 shows the stiffness decay curves of beams C4 and C5 over the full fatigue history. This figure describes the stiffness degradation law during the entire process of fatigue failure. Beams C4 and C5 experience a complete fatigue failure process, and data show that with the development of load history, the stiffness degradation exhibits distinct three-stage characteristics. In the initial stage of fatigue loading and the two stages before the adjacent failure, the stiffness decreases remarkably. In the 0.2 times life period, the stiffness degenerates to about 0.6–0.7, which is in linear stage of stable development and gentle decline in the middle and longer period. In the following figures, N represents the fatigue life of the beam, and n represents loading times in the fatigue test.

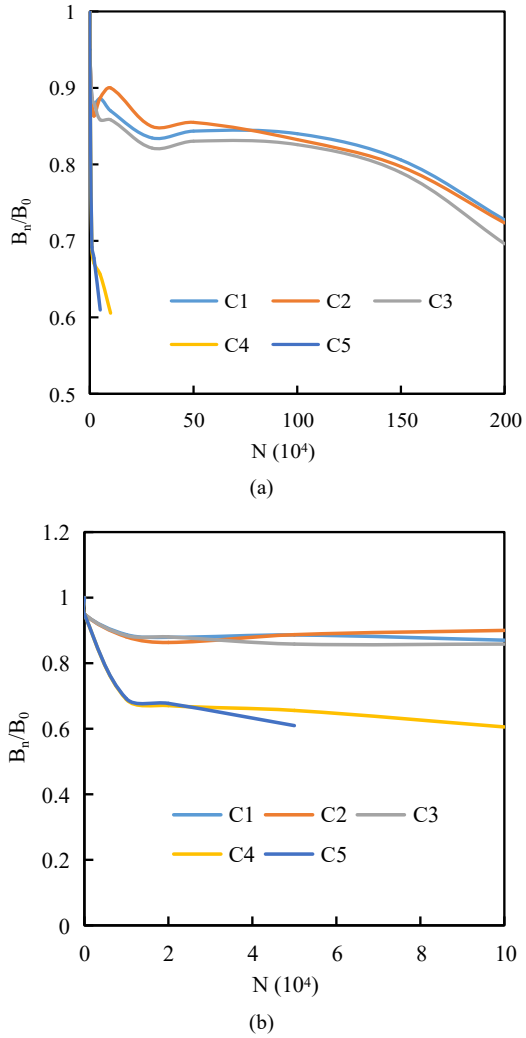

Fig. 5 The law of stiffness attenuation of components. (a)Decay law of beam stiffness in constant amplitude fatigue test (b)Attenuation law of test beam stiffness after 100,000 times of fatigue loading.

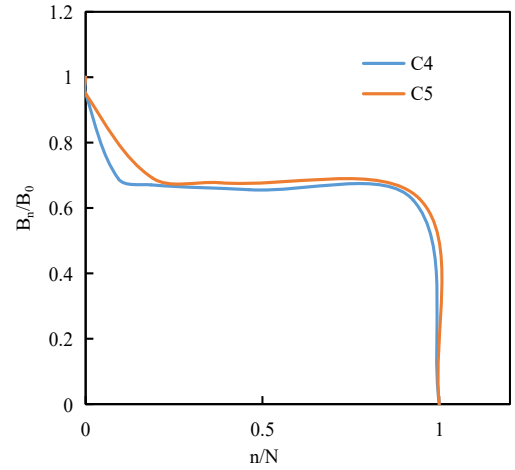

Fig. 6 Stiffness degradation in the whole process of constant-amplitude fatigue test.

The attenuation law of section stiffness can be obtained from the load–concrete compressive strain data, and the stiffness attenuation coefficient is defined as B_c / B_{c0}. B_c represents the section stiffness of the member after the times of fatigue loading, and B_{c0} represents the initial section stiffness defined in terms of concrete strain.

In the 1st and 2nd stages of fatigue loading, the decay curves of the section stiffness of the test beams are shown in Figure 7. Increasing fatigue loading times results in continuously decreasing section stiffness. When the lower limit of fatigue loading is the same, the higher the upper limit of fatigue loading is, the faster the stiffness decays. Figure 7(b) shows that the attenuation coefficients of the stiffness of beams C1, C2, and C3 after 100,000 fatigue loadings decrease by 5.6%, 7.4%, and 20%, respectively. Beams C4 and C5 have loaded 10,000 times that of fatigue loading and have attenuation coefficients of 0.44 and 0.61, respectively, with a decrease of 37% and 55%, respectively. This result shows that under equivalent fatigue load, the structural stiffness decay rate under heavy load is significantly higher than that under normal operating load.

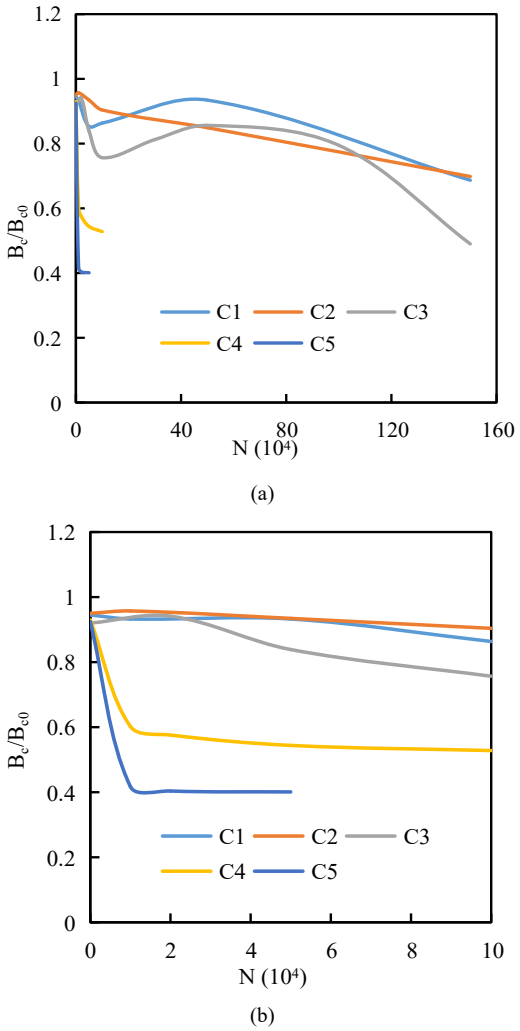

Fig. 7 Section stiffness characterized by concrete strain. (a) 1.5 million times (b) 100,000 time.

Beams C4 and C5 have experienced a complete fatigue failure process, and the section stiffness decay curves of their entire life cycle are shown in Figure 8. In the complete fatigue load history, the change curve of the stiffness coefficient of the test beam section with fatigue failure is S-shaped, and the three-stage division is evident. The section stiffness decays rapidly in the first stage of fatigue loading (about 10%–20%), decreases gently in the second stage (about 80%), and decays rapidly again until the beam body fails in the third stage (about 10%). In the figure, N represents the fatigue life of the beam, and n represents the number of loadings in the fatigue test.

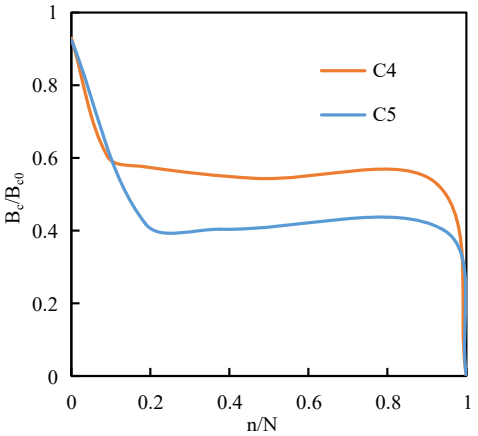

Fig. 8 Degradation of section stiffness in the whole process of test beam fatigue.

According to the strain change data of the nonprestressed tendon, the stiffness attenuation coefficient B_s / B_{s0} curve defined by the nonprestressed tendon strain can be drawn as shown in Figure 9(a). B_s represents the stiffness after the times of fatigue loading, and B_{s0} represents the initial section stiffness defined by ordinary reinforcement strain.

Similarly, the curve of the stiffness attenuation coefficient B_p / B_{p0} defined by the strain of the prestressed tendon can be drawn in accordance with the strain change data of the prestressed tendon, as shown in Figure 9(b). B_p represents the stiffness of the component after the times of fatigue loading, and B_{p0} represents the initial stiffness.

Figure 9(a) shows that the stiffness decay law defined by the nonprestressed steel strain decreases continuously with increasing number of fatigue loadings. A large upper limit of fatigue loading results in fast stiffness decay rate, and the overall change presents stages, which are consistent with the stiffness decay law defined by the concrete strain. Figure 9(b) shows that the stiffness decay law of prestressed steel bars decreases with increasing fatigue loading times, which may be due to the development of the law of nonprestressed steel bars. The comparison of the test beams under different working conditions shows that under the equivalent fatigue load, a high loading upper limit results in fast section stiffness degradation of the test beam.

Component stiffness refers to the ability of a component to resist deformation, that is, the ratio of the internal force caused by the force applied to the component to its corresponding component deformation. Section stiffness refers to the ability of the section to resist deformation, and the expression of section bending stiffness is the product of the material's modulus of elasticity and the corresponding moment of inertia of the section. From the previous discussion, we know the law of member stiffness attenuation. Therefore, this section uses the member stiffness as the benchmark to compare the section stiffness data of each test beam and find optimal parameters that can express the cumulative degradation process of the test beam fatigue damage.

The relationship between section stiffness and member stiffness is analyzed, and the overall section stiffness and member stiffness are exponentially fitted (Figure 10).

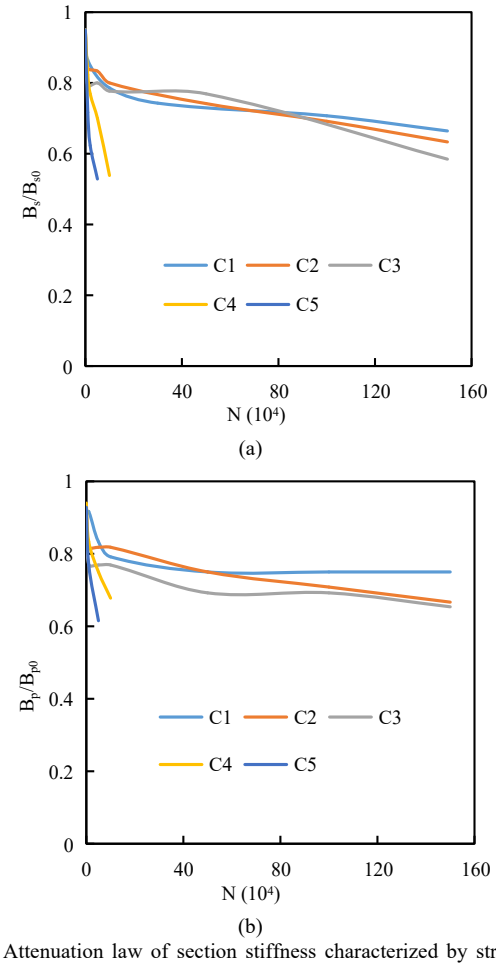

Fig. 9 Attenuation law of section stiffness characterized by strain. (a) Non-prestressed tendon strain (b) Prestressing tendon strain.

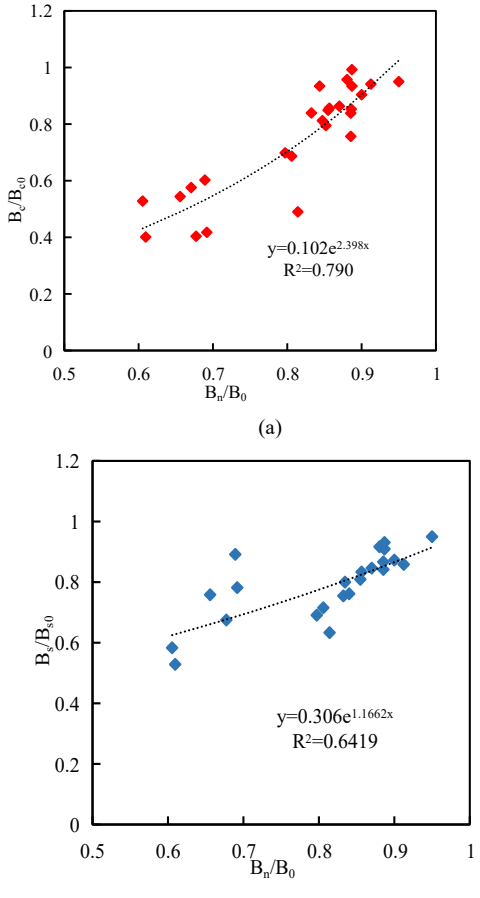

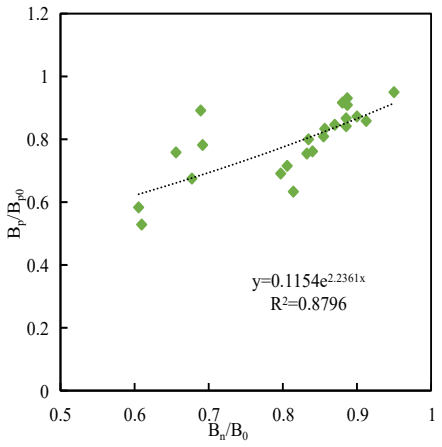

(c)

Fig.10 Overall Correlation Between Section Stiffness and Member Stiffness. (a) Concrete. (b) Non-prestressed tendons (c) Prestressed reinforcement.

A comprehensive comparison of the cross-sectional stiffness correlation coefficients (Fig. 10) characterized by the strain of each material shows that the cross-sectional stiffness coefficients of each material are positively correlated with member stiffness. The correlation between the section stiffness coefficient of the steel bar and the member stiffness coefficient is the worst, the concrete correlation is general, and the stiffness correlation represented by the prestressed steel bar is best. The minimum stiffness principle theory elaborates that within the full-span length of a simply supported beam, the deflection can be calculated in accordance with the minimum bending stiffness of the section by using a formula in material mechanics that does not consider the influence of shear deformation. Therefore, the cumulative damage process of prestressed concrete beams under heavy load fatigue can be expressed using the section stiffness coefficient represented by the strain of prestressed tendons.

5. Conclusions

This study aimed to explore the stiffness degradation law of prestressed concrete beams under the equivalent fatigue load and reveal the relationship between the member's section stiffness and member stiffness. This study started with the determination of the equivalent fatigue load, used a combination of data statistics and experimental research, and analyzed the fatigue deformation characteristics and section material properties of prestressed concrete beams. The following conclusions could be drawn.

(1) The final failure mode of the prestressed concrete beam starts from the bending failure of the fatigue fracture of the ordinary steel bar under longitudinal tension at the bottom of the beam. The main cracks of the test beam are mostly near the mid-span.

(2) During the fatigue test, the stiffness of the test beam shows a three-stage decay trend of "fast–gentle–fast" with increasing fatigue loading times. The stiffness attenuation coefficient of steel bars can characterize the stiffness attenuation characteristics of prestressed concrete beams. The section stiffness characterized by the prestressed tendon strain has the best correlation with the member stiffness of the prestressed concrete beam and can be used as a characterization parameter to express the prestressed concrete beam's cumulative damage process under heavy load fatigue.

Thus, this study combines laboratory experiments with mathematical statistics and proposes the law of stiffness degradation under equivalent fatigue loads. The proposed characterization parameters are close to the actual situation in the field and have a certain reference for the action mechanism under the actual vehicle load. Given the lack of data on on-site environmental factors, the environmental monitoring data are combined with the test components in future research to have an accurate understanding of the fatigue damage characteristics of prestressed concrete beams.

Acknowledgements
This work was supported by the Science and Technology Project of Hebei Education Department (BJ2019042), the Advanced Talents Incubation Program of the Hebei University (521000981264), and the Excellent Experimental Project of Hebei University (2021-BZ-JPSY16).

References

1. Ministry of railways of the people's republic of China. "*Code for design of prestressed concrete structures JGJ369-2016*". Beijing: China Architecture and Building Press, China, 2016.129.p.
2. Yang O., Zhang XF., Huo JS., Chen, J., "Research status of fatigue performance of prestressed concrete beam". *Journal of Architecture and Civil Engineering*, 34(4), 2017, pp.85-89.
3. Raithby, K. D., "Fatigue of steel and concrete structures: Proceedings of the IABSE Colloquium, Lausanne, 1982 IABSE Reports AK37(1982)". *International Journal of Fatigue*, 5(3), 1983, pp.180-181.
4. Xin, Q., Dou, Y. M., Zhang, J. J., Li, S., "Deflection calculation of partially prestressed concrete beams under heavy duty". *DYNA*, 93, 1999, pp.301-307.
5. Xin, Q., Dou, Y. M., Ma, N. J., Xin, Y. N., "Influence of environment corrosion on the fatigue performance of expressway bridges". *Journal of Engineering Science and Technology Review*, 10(1), 2017, pp. 1-9.
6. Zhang, J. J., Dou, Y. M., Xiao, X. N., "The analysis of fatigue performance and engineering cost of partial pre-stressed concrete beam". *Industrial Safety and Environmental Protection*, 44(1), 2018, pp.50-54.
7. Zhang, J. J., Xin, Q., Yang, Y. X., Dou, Y. M., "Research on bending behavior of corroded ppc beams strengthened by external pre-stressing". *Industrial Construction*, 48(9), 2018, pp.198-203.
8. Vaško, M., Handrik, M., Rác, M., Baniari, V., Kortiš, J., Daniel, Ľ. Ján, K., Ľuboš, D., "The damage analysis of the reinforced concrete beam and the prestressed reinforced concrete beam". *MATEC Web of Conferences*, 157, 2018, pp.1-10.
9. Wang, C., Liu, Q., Dang, Z., "Deflection-based analysis of prestress loss for continuous girder bridges". *China Water Transport*, 2021, pp.154-156.
10. Zhou, T. Q., Chen, H. T., "Fatigue damage accumulation analysis of long-span steel bridge members based on damage mechanics-finite element method". *Ship Mechanics*, 2009, pp. 739-747.

11. Allawi, A. A., "Behavior of strengthened composite prestressed concrete girders under static and repeated loading". *Advances in Civil Engineering,* 2017, pp. 1-13.
12. Allawi, A. A., "Flexural performance of laced reinforced concrete beams under static and fatigue loads". *Journal of Engineering,* 25(10), 2019, pp.134-153.
13. Qiao, P., "Research on Prediction Method of Bridge Stiffness Performance Degradation Based on Grey Theory". *North Traffic*, 2021, pp.18-21.
14. Garavaglia, E., Pavani, R., Sgambi, L., "The Use of Fragility Curves in the Life-Cycle Assessment of Deteriorating Bridge Structures". *Computation,* 9(3), 2021, pp. 25.
15. OBrien, E. J., Bordallo-Ruiz, A., Enright, B., "Lifetime maximum load effects on short-span bridges subject to growing traffic volumes". *Structural Safety*, 50, 2014, pp. 113-122.
16. OBrien, E. J., Enright, B., "Modeling same-direction two-lane traffic for bridge loading". *Structural Safety*, 33(4), 2011, pp.296-304.
17. Wang, S. W., Chen, S. Q., Song, X. D., "Research on fatigue performance of combined beam bridge based on vehicle-axle coupled vibration". *Railway Building*, 2020, pp.90-92.
18. Xu, Y. C., Zhang, Y. F., Ding Y.X., Yang, C., "Analysis of traffic distribution characteristics of highway bridges based on actual measurement". *Traffic World*, 2020, pp.90-92.
19. Zhou, H. Y., Zhou, Y., Liu, Y. N., Tang. Q., "Degradation of Fatigue Bending Stiffness of Prestressed Concrete Beams Considering Size Effect". *Industrial Building*, 51 (11), 2021, pp. 62-66.
20. Nesterova, M., Schmidt, F., Soize, C., "Fatigue analysis of a bridge deck using the peaks-over-threshold approach with application to the Millau viaduct". *SN Applied Sciences*, 2(8), 2020, pp.1416.
21. Bertolesi, E., Buitrago, M., Adam, J.M. and Calderon, P.A., "Fatigue assessment of steel riveted railway bridges: Full-scale tests and analytical approach". *Journal of Constructional Steel Research*, 182, 2021, pp.106664.
22. Li, M. W., "Damage Index Calculation of Continuous Rigid Frame Bridges Based on Stiffness Degradation Model". *Green Environmental protection Building Materials*, (03), 2020, pp.142-143.
23. Zhang, H. B., Chen, R., "Influence of congenital defects on stiffness of long-span prestressed concrete continuous bridges". *Western China Communications Science & Technology*, (04), 2019, pp.139-141.
24. Du, Y., Wei, J., Yuan, J., Lai, Y. F., Sum, D. H., "Experimental research on fatigue behavior of prestressed concrete beams under constant-amplitude and variable-amplitude fatigue loading". *Construction and Building Materials*, 259, 2020, pp.119852.
25. Xu, J. J., Zhu, P., Ma, Z. J., Qu, W. J., "Fatigue flexural analysis of concrete beams reinforced with hybrid GFRP and steel Bars". *Engineering Structures*, 199, 2019, pp.109635.
26. Gao, R. Y., Xin, Q., Hu, X. Q., Liang C.Y., "Residual performance analysis of bridge structure considering heavy load effect". *DYNA*, 97, 2022, pp.156-161.
27. Ministry of housing and urban-rural construction of the people's republic of China and general administration of quality supervision "*Standard for test method of concrete structures. GB/T 50152-2012*". Beijing: China Architecture and Building Press, China, 2012, pp. 119.